Letters

Nonlinear Coupled Inductor-Based Light-Load Efficiency Boost Technique for Trans-Inductor Voltage Regulators

Zehui Li, Jiawei Liang, Minfan Fu, *Senior Member, IEEE*, Teng Long, *Member, IEEE*, and Haoyu Wang, *Senior Member, IEEE*

***Abstract*—Trans-inductor voltage regulator (TLVR) exhibits good scalability and easy multiphase magnetic coupling, making it an optimal choice for high-current point-of-load (PoL) solutions in modern data centers. Meanwhile, data center servers work at light load for the majority of their operating time, so it is imperative to improve the light-load efficiency of PoL converters. The phase-shedding (PS) technique is a simple and effective method for improving light-load efficiency in multiphase PoL converters. However, heavy coupling between phases in TLVR degrades its effectiveness. To address this issue, we propose a novel nonlinear coupled inductor (CL) for TLVR to enhance its compatibility with PS technique, improving light-load efficiency. At light load, the nonlinear CL exhibits light coupling and increased inductance, effectively decoupling the phases and minimizing ripple current. A detailed analysis of the light-load efficiency and magnetic design considerations is provided. A four-phase 12 V-to-1.8 V, 80 A TLVR incorporating the proposed nonlinear CL is designed and tested. Experimental results demonstrate an improvement in light-load efficiency compared with systems utilizing linear CLs, with a maximum efficiency improvement of 2.5%.**

***Index Terms*—Light-load efficiency, magnetic design, nonlinear inductor, trans-inductance, voltage regulator.**

I. Introduction

With the rapid evolution of modern information technologies, data center power consumption is booming and is expected to reach 8% of global electric power consumption by 2030 [1]. Typically, data centers in enterprises only consume 5%–15% of rated power on average [2]. Furthermore, over 89% of the server operation experiences power consumption below 10% of the rated capacity. That is, the power supply operates mainly under standby and light-load conditions [2]. Therefore, improving the light-load efficiency is crucial for energy saving in data centers.

The load point voltage in data centers is trending downward, reaching sub 1V [3]. As microprocessors integrate an increasing number of transistors, this surge in density increases the demand for the output current, which now exceeds 220 A, as detailed in [4] and [5]. Such a "low voltage, high current" scenario imposes significant challenges to the optimal design of the point-of-load (PoL) converters [4], [5], [6], [7]. To achieve a large output current, multiphase structure is often adopted in PoL applications [5]. In recent years, due to the scalability and ease of magnetic components production, multiphase Trans-inductor voltage regulator (TLVR) has garnered increasing interest within the industry [7], [8].

For multiphase PoL converters, phase-shedding (PS) technology [9], [10] is a common and effective method for improving light-load efficiency. The core idea is to reduce the number of active phases during light-load operation. To achieve a fast transient response at full load, the coupling coefficient of multiphase TLVR is high. When PS is carried out in TLVR, due to the strong coupling between phases, coupled currents still flow through the inactive phases, diminishing the efficiency boost from PS technology. Therefore, a nonlinear coupled inductor (CL) with weak coupling at light load and strong coupling at heavy load can solve the dilemma.

Several nonlinear CLs with adaptive coupling coefficient are investigated [11], [12], [13], [14]. In [11], extrinsic material is inserted into the gap of the central leg of "EI" core to form the nonlinear CL. The added part saturates at heavy load. This facilitates an adaptive inductance and coupling coefficient. A planar nonlinear CL is introduced in [12] and [13], consisting of two planar windings and three-layer magnetic cores made of two different materials. The coupling coefficient remains low at light load. With the load current rises, the middle layer composed of high permeability material, gradually saturates, and the coupling becomes heavier. In [14], three distinct magnetic materials construct the nonlinear CL. The coupling coefficient dynamically adjusts with the load power. Nevertheless, the differences in magnetic permeability of the various materials applied limit the

Received 23 January 2025; revised 17 March 2025, 25 April 2025, and 19 May 2025; accepted 5 June 2025. Date of publication 11 June 2025; date of current version 5 August 2025. This work was supported by the National Natural Science Foundation of China under Grant 52077140. *(Corresponding author: Haoyu Wang.)*

Zehui Li, Jiawei Liang, Minfan Fu, and Haoyu Wang are with the Power Electronics and Renewable Energies Laboratory, School of Information Science and Technology, ShanghaiTech University, Shanghai 201210, China, and also with the Shanghai Engineering Research Center of Energy Efficient and Custom AI IC, Shanghai 201210, China (e-mail: lizh2@shanghaitech.edu.cn; liangjw@shanghaitech.edu.cn; fumf@shanghaitech.edu.cn; wanghy@shanghaitech.edu.cn).

Teng Long is with the Electrical Engineering Division, Department of Engineering, University of Cambridge, CB3 0FA Cambridge, U.K. (e-mail: tl322@cam.ac.uk).

Color versions of one or more figures in this article are available at https://doi.org/10.1109/TPEL.2025.3578947.

Digital Object Identifier 10.1109/TPEL.2025.3578947

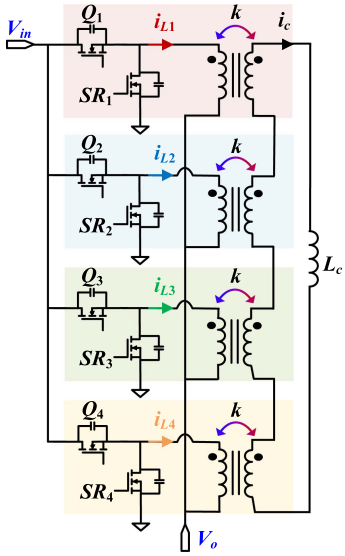

Fig. 1. Schematic of a four-phase interleaved TLVR based on proposed nonlinear CLs.

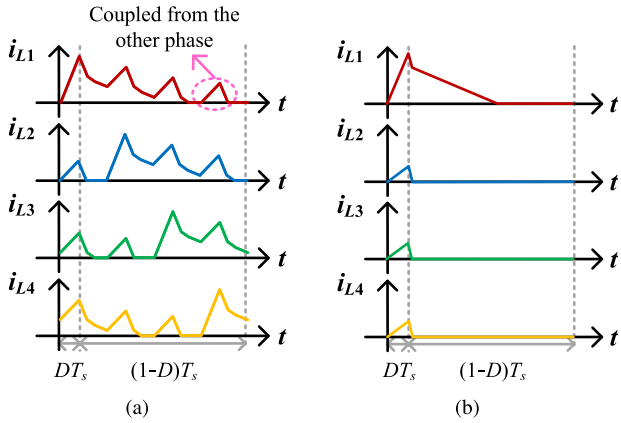

Fig. 2. Inductor current waveforms in DCM. (a) four-phase interleaving. (b) With PS.

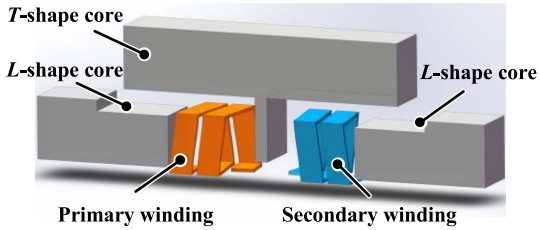

Fig. 3. Exploded view of the nonlinear CL.

range of parameter variation. The range of coupling coefficient of the nonlinear CL proposed in [12] is just from -0.205 to -0.421. This limitation prevents full decoupling at light loads. Thus, they cannot adequately demonstrate the efficiency improvement of PS technology. Few studies focus on the combination of the nonlinear properties and the PS technology, which can enhance the boost of light-load efficiency for TLVR.

In this letter, we propose a novel nonlinear CL featuring a broad spectrum of coupling coefficients for multiphase TLVR. The proposed nonlinear CL is not constrained by material limitations. It provides separate paths for the primary and secondary fluxes, enabling nearly complete decoupling under light-load conditions. This design enhances light-load efficiency while preserving low transient inductance during heavy loads. A schematic illustration of a four-phase application is presented in Fig. 1. The advanced inductor design permits the coupling coefficient to attain near-zero values, effectively minimizing power losses from interphase coupling at light loads. Notably, this capability for complete decoupling markedly simplifies the implementation of PS, thereby further improving light-load efficiency.

This refinement not only optimizes performance across different load scenarios but also contributes to a more straightforward converter design and operation.

II. Light-Load Analysis

At light load, where the load current is lower than 20% of the full load, TLVR enters into discontinuous conduction mode (DCM), its critical waveforms are shown in Fig. 2(a). In DCM, when the current in one phase (e.g., phase 1) drops to zero, a coupling current from an active phase (e.g., phase 4) flows into this inactive phase. This coupling current freewheels through the body diode of the inactive phase synchronous rectifier (SR), causing a significant conduction loss and reduced efficiency. This phenomenon also exists when PS [9], [10] is used to further improve the light-load efficiency, as demonstrated in Fig. 2(b). To maintain high light-load efficiency, it is crucial to avoid body diode conduction.

One way is to turn ON the SRs actively to reduce the conduction loss. However, this introduces additional driving loss and increases the complexity of the control. Another way is to decouple the phases to eliminate the coupling current at light loads. However, strong coupling of the TLVR is required to achieve a fast transient response during sudden load changes. Therefore, a nonlinear CL with variable coupling is preferable. At light load, the coupling is mitigated to improve the light-load efficiency. As the load increases, the coupling is enhanced to maintain the transient performance.

III. Design of Nonlinear CL

The nonlinear CL exhibits a low coupling coefficient at light load. As the load increases, the coupling coefficient of the nonlinear CL gradually increases. This nonlinear characteristic can be realized through the partial saturation of the magnetic core. In CLs, the coupling coefficient is influenced by the path of the magnetic flux. Magnetic core saturation alters this flux path, thereby modifying the coupling coefficient. Therefore, the key to realizing the nonlinear feature is a magnetic core with a controllable saturation degree. The proposed nonlinear CL integrates two L-shape cores and one T-shape core, as shown in Fig. 3. The primary winding and the secondary winding are separately wound on two L-shaped cores. Finite element analysis

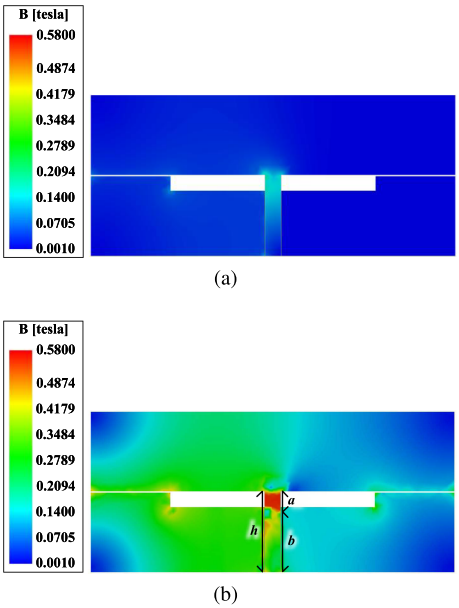

Fig. 4. Finite element simulation of DC flux density for the nonlinear CL. (a) Light load. (b) Full load.

(FEA) simulation results of dc flux density at both light and heavy loads are shown in Fig. 4, illustrating how saturation of the central leg alters the magnetic flux path. The middle of the T-shape core tends to saturate as the load increases.

The design methodology for the proposed nonlinear CL is depicted in Fig. 5, illustrating the step-by-step process to achieve the desired magnetic properties. L_{ss_heavy}, L_{ss_light}, k_{heavy}, and k_{light} are the equivalent steady-state inductance and coupling coefficient at heavy and light loads, respectively. Through reluctance modeling, the mathematical relationship between core size and design objectives can be obtained. Based on the magnetic model, the appropriate dimensions can be selected to meet the design requirements. Especially, the magnetic reluctance of the middle of the T-shape core is different at light load and heavy load, since this part will saturate at heavy load, as shown in the following:

$$R_{\text{light}} = \frac{h}{\mu A} \tag{1}$$

$$R_{\text{heavy}} = \frac{a}{\mu A} + \frac{b}{\mu_{\text{sat}} A} \tag{2}$$

where a is the length of core that does not saturate, b is the length of the saturated part, and h is the length of the middle of T-shape core, as shown in Fig. 4(b). Obviously, $a + b = h$. μ_{sat} is the permeability of the saturated part. A is the cross-sectional area of T-shape core. The actual a and b can be obtained from the FEA simulation.

The picture of the nonlinear CL is shown in Fig. 6. The material is DMR95, and the nonlinear feature during steady state is shown in Fig. 7. The inductance of each CL when the coupled winding loop is open, L_{nc} gradually decreases from 1.03 μH to about 580 nH. Larger inductance at light load can reduce the

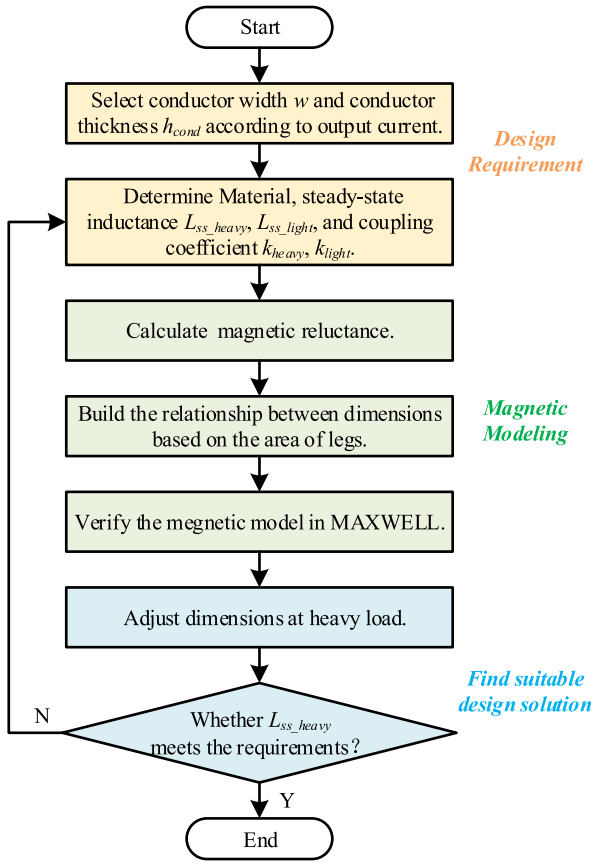

Fig. 5. Flowchart of magnetic design.

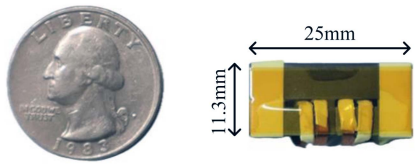

One quarter dollar

Fig. 6. Picture of nonlinear CL.

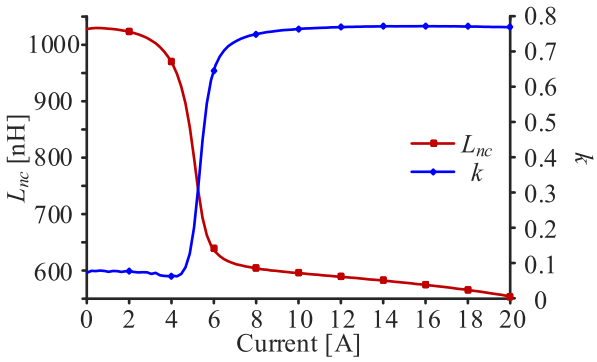

Fig. 7. Inductances and coupling coefficients at steady state.

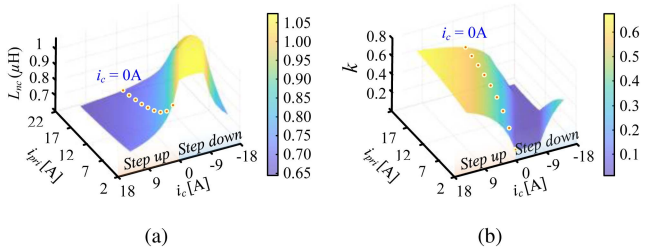

(a) (b)

Fig. 8. Inductances and coupling coefficients at transient conditions. (a) Self-inductance L_{nc}. (b) Coupling coefficient k.

current ripple-induced loss, such as the conduction loss and ac winding loss. Coupling coefficient $|k|$ increases from 0.08 to 0.77 as phase current increases from 2 to 20A. The threshold of the nonlinear CL is defined by the load range. When the output current is 16 A (light-load condition), the four-phase TLVR distributes 4 A per phase. To enhance light-load efficiency, the nonlinear CL must reduce the coupling coefficient at 4 A.

Fig. 8(a) illustrates the simulation results of inductance variation during transient conditions, and Fig. 8(b) shows the variation of the coupling coefficient k. During transient conditions, a bias is generated in i_c [7]. When $i_c = 0$, it corresponds to the steady-state results. When the load steps up, i_c intensifies the saturation of the central leg, resulting in reduced inductance. The greater the load increase, the smaller the inductance. Simultaneously, k increases. Conversely, when the load steps down, i_c weakens the saturation of the central leg, causing an increase in inductance. The larger the load steps down, the greater the inductance, while k decreases. Eventually, when i_c becomes large enough to saturate the central leg, the inductance decreases again, and k increases.

IV. Discussion on the Influence of Nonlinear CLs

A. System Stability Analysis

To analyze the impact of nonlinear CLs on system stability, a SIMPLIS-based simulation platform is developed. A constant-on-time control loop with a type 2 error compensator is designed for the four-phase TLVR with nonlinear CLs to enhance transient response [15]. The closed-loop control structure, as shown in Fig. 9(a), comprises a current loop and a voltage loop. The current loop senses the overall inductor current via resistor R_i, while the voltage loop employs a type 2 compensator to ensure stability under high-bandwidth operation.

The closed-loop control-to-output transfer function, G_{vc}, is illustrated in Fig. 10(a). Fig. 10 illustrates the Bode plots within the load range of 12 A (light load) to 80 A (full load). The measured conditions fully cover the variation range of nonlinear CLs. As shown in Fig. 10(a), the phase margin of G_{vc} is between 94.78° and 96.37°.

However, the influence of nonlinear CLs on system behavior cannot be directly assessed via Bode plots. In contrast, time-domain simulations provide clearer insights into stability during load transients. As shown in Fig. 11, when the output current abruptly steps from 10 to 80 A, the output voltage exhibits

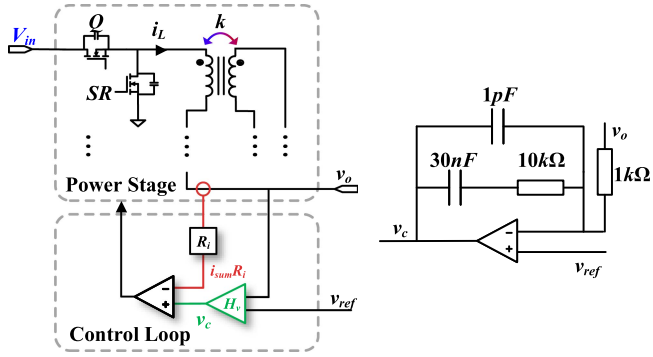

(a) (b)

Fig. 9. Closed-loop control. (a) Control diagram. (b) Design of the type 2 compensator.

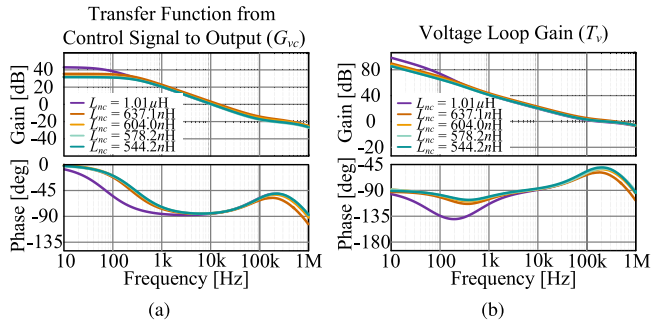

(a) (b)

Fig. 10. Closed-loop transfer function. (a) Control-to-output (G_{vc}). (b) Voltage-loop gain (T_v).

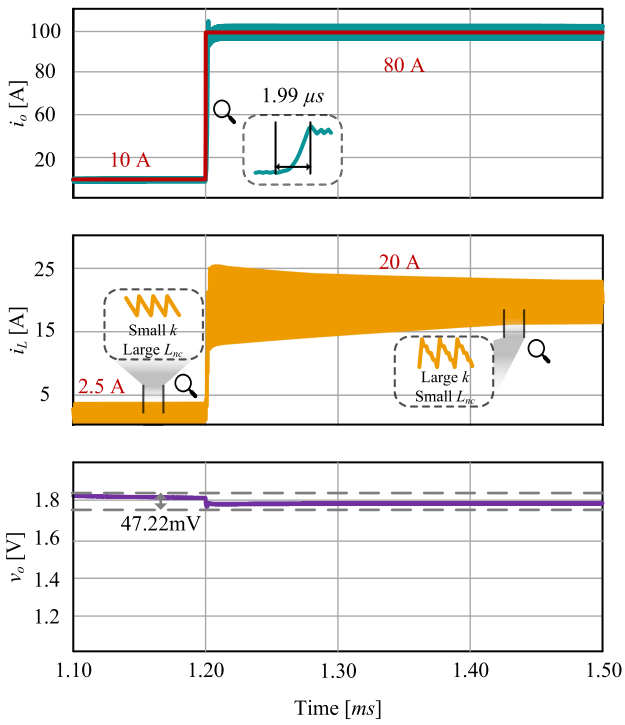

Fig. 11. Simulation results during transient process.

TABLE I
SPECIFICATION OF THE CLS

Quantity	Nonlinear CL	Constant CL
Footprint	25 × 4.25 mm	25 × 6 mm
Height	11.3mm	12.8 mm
L_{nc}	1.03μ H – 580 nH	595 nH
k	0.08 – 0.77	0.72
Inflexion point	4 – 6 A	$\gg$ 20 A
Winding	2.5 × 0.3 mm	2.5 × 0.3 mm

a transient fluctuation of approximately 47.22 mV but rapidly recovers to its rated value. Notably, the nonlinear CL undergoes full parameter variation across the 10–80 A load transient range. This result confirms system stability, with no output voltage oscillation during load variations.

B. Transient Response

The parameter design of the control loop significantly influences the transient response. The transfer function of the type 2 compensator is in the following:

$$H_v = A_v \frac{(1 + s/\omega_z)}{s(1 + s/\omega_p)}. \tag{3}$$

The parameters of H_v are set as: $A_v = 90.457$ dB, $f_z = \omega_z /2\pi = 530.516$ Hz, and $f_p = \omega_p /2\pi = 15.915$ MHz. The design of type 2 compensator is shown in Fig. 9(b).

The voltage-loop gain, T_v, is shown in Fig. 10(b). The designed closed-loop control achieves a cutoff frequency range of 235–422 kHz. Meanwhile, the phase margin of the system is between 108° and 128.58°, indicating that the system is stable.

The simulated transient waveforms are captured in Fig. 11. When the load changes from 10 to 80 A, the response time is 1.99 μs. The reduced inductance of the nonlinear CL increases current ripple during the load step-up transient. Under equivalent full-load inductance conditions, the four-phase conventional TLVR achieves a marginally faster transient response (1.46 μs) compared to the nonlinear CL-based TLVR. However, the proposed design enables decoupling at light loads, reducing current ripple and dramatically improving light-load efficiency. This marginal tradeoff in transient performance is deemed acceptable.

In addition, load transient simulations were performed in SIMPLIS across frequencies ranging from 1 to 500 kHz and duty cycles from 10% to 90%. Results indicate that during load step-down transients, the maximum output voltage remains below 1.85 V, while during load step-up transients, the minimum output voltage is higher than 1.75 V.

V. EXPERIMENTAL VALIDATION

To compare the effect of the proposed nonlinear CL, a constant CLs with identical material is designed. The parameter comparison between the two CLs is given in Table I.

A four-phase 12 V/1.8 V/80 A 500 kHz TLVR with nonlinear CLs is designed for experimental validation. The photograph of the test setup and the prototype is shown in Fig. 12. Two efficiency curves are captured in Fig. 13, with the load current changing from 80 to 4 A. At heavy loads, the efficiency of the

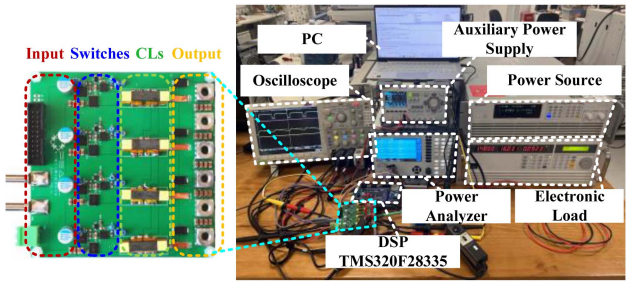

Fig. 12. Picture of the prototype and the experiment setup.

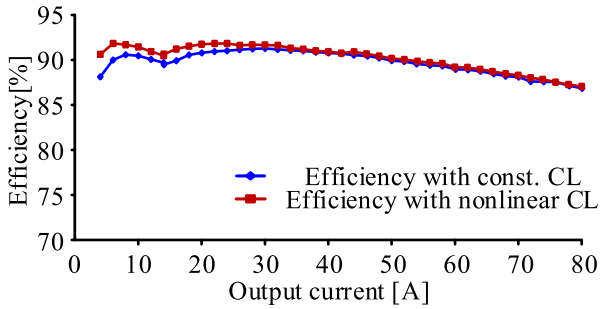

Fig. 13. Efficiency curves with constant CL and nonlinear CL.

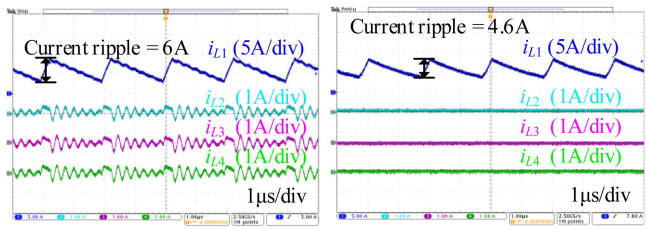

(a) (b)

Fig. 14. Experiments waveforms at 6 A output current (PS). (a) TLVR with constant CLs. (b) TLVR with nonlinear CLs.

TLVR with constant CLs and the proposed nonlinear CLs is almost the same. As the load decreases, efficiency with constant CLs improves, due to the reduced current ripple. When it is less than 16 A, PS is carried out to further improve light-load efficiency. For TLVR using nonlinear CLs, the efficiency at full load is 87.06%, and the peak efficiency appears around 6 A, which is 91.84%. Compared to traditional solutions, the operating efficiency at light loads has increased by up to 2.5%.

Fig. 14(a) shows the PS currents of TLVR with constant CL, where only Phase 1 is active. The current ripple of Phase 1 is about 6 A. The inactive phases carry a part of the output current, revealing that TLVR with constant CL cannot achieve perfect PS. As shown in Fig. 14(b), TLVR with the proposed nonlinear CL can almost completely decouple the four phases, with almost no coupling current in the inactive phases. The current ripples are smaller, which are 4.6 A.

Fig. 15(a) captures the open-loop transient waveforms for a 30–60 A load step. During this transient, the current ripple (Δi) increases due to a positive current bias in i_c, which strengthens interphase coupling. Conversely, Fig. 15(b) depicts the 60–30 A

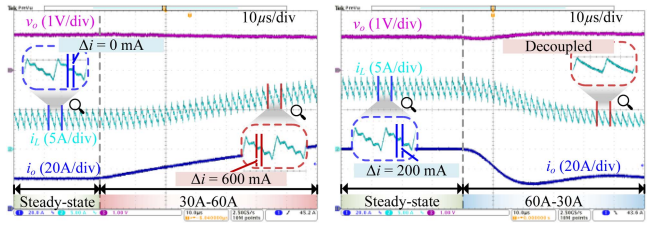

(a) (b)

Fig. 15. Open-loop transient waveforms during (a) step-up transient from 30 to 60 A and (b) step-down transient from 60 to 30 A.

transient, where Δi decreases as a negative current bias in i_c and reduces central leg saturation, nearly decoupling the phases. These open-loop transients corroborate the nonlinear behavior, as illustrated in Fig. 8.

VI. Conclusion

To boost the light-load efficiency of CL-based multiphase converters in data center applications, this letter proposes a novel nonlinear CL that has a smaller coupling coefficient and larger inductance at light load, while maintaining a smaller inductance and larger coupling coefficient at heavy load. A 12/1.8 V, 80 A, 500 kHz, four-phase TLVR is designed and tested. A constant CL with parameters similar to those of the nonlinear one at heavy load is designed for comparison. The experimental results show that the proposed nonlinear CL can effectively improve the light load efficiency of TLVR without significantly sacrificing the heavy load efficiency, achieving a maximum efficiency improvement of approximately 2.5%.

Acknowledgment

The authors would like to thank Hengdian Group DMEGC Magnetics for customizing the ferrite core samples for this research.

References

[1] S. Clement, K. Burdett, N. Rteil, A. Wynne, and R. Kenny, "Is hot IT a false economy? An analysis of server and data center energy efficiency as temperatures rise," *IEEE Trans. Sustain. Comput.*, vol. 9, no. 3, pp. 482–493, May/Jun. 2024.

[2] J. Liang and H. Wang, "Light load efficiency boost technique for switched tank converters based on hybrid ZVS-ZCS control," in *Proc. Int. Power Electron. Conf.*, Himeji, Japan, May 2022, pp. 2231–2235.

[3] H. Wu, Y. Song, X. Zhang, and Y. Zhang, "Current-cancellation-based heterogeneous integration of LLC-DCX with ultralow-voltage high-current output for data centers," *IEEE Trans. Power Electron.*, vol. 39, no. 8, pp. 9144–9149, Aug. 2024.

[4] J. Liang, L. Wang, M. Fu, J. Liang, and H. Wang, "Overview of voltage regulator modules in 48 V bus-based data center power systems," *CPSS Trans. Power Electron. Appl.*, vol. 7, no. 3, pp. 283–299, Sep. 2022.

[5] X. Lou and Q. Li, "Single-stage 48 V/1.8 V converter with a novel integrated magnetics and 1000 W/in^3 power density," *IEEE Trans. Ind. Electron.*, vol. 71, no. 7, pp. 6601–6611, Jul. 2024.

[6] Y.-S. Hwang, J.-J. Chen, Y.-T. Ku, and J.-Y. Yang, "An improved optimum-damping current-mode buck converter with fast-transient response and small-transient voltage using new current sensing circuits," *IEEE Trans. Ind. Electron.*, vol. 68, no. 10, pp. 9505–9514, Oct. 2021.

[7] F. Zhu and Q. Li, "Coupled inductors with an adaptive coupling coefficient for multiphase voltage regulators," *IEEE Trans. Power Electron.*, vol. 38, no. 1, pp. 739–749, Jan. 2023.

[8] H. Shao, T. Zhao, D. Fu, D. Huang, and J. Zhou, "Analytic model and design procedure of the single-secondary trans-inductor voltage regulator," in *Proc. IEEE Energy Convers. Congr. Expo.*, Vancouver, BC, Canada, Nov. 2021, pp. 2005–2010.

[9] J.-T. Su and C.-W. Liu, "A novel phase-shedding control scheme for improved light load efficiency of multiphase interleaved DC–DC converters," *IEEE Trans. Power Electron.*, vol. 28, no. 10, pp. 4742–4752, Oct. 2013.

[10] G. Son, Z. Huang, and Q. Li, "Light load efficiency improvement for two-channel paralleled soft-switching three-phase inverter using phase shedding control," *IEEE Trans. Power Electron.*, vol. 37, no. 9, pp. 10200–10212, Sep. 2022.

[11] X. Liang, M. Wang, H. Tamdem, and N. Ahuja, "A novel coupled inductor to improve performance of voltage regulators in computing system," in *Proc. IEEE Appl. Power Electron. Conf. Expo.*, New Orleans, LA, USA, Jun. 2020, pp. 506–511.

[12] F. Li, L. Wang, B. Wu, L. Yu, and K. Wang, "A novel planar nonlinear coupled inductor for improving light and intermediate load efficiency of DC/DC converters," *IEEE J. Emerg. Sel. Topics Power Electron.*, vol. 11, no. 2, pp. 2004–2014, Apr. 2023.

[13] L. Yu, C. Wang, H. Cui, Y. Gan, and L. Wang, "A 3D integrated nonlinear inductor for improving light load efficiency of voltage regulator modules," in *Proc. IEEE Appl. Power Electron. Conf. Expo.*, Houston, TX, USA, May 2022, pp. 1043–1047.

[14] M. Ishigaki, K. Shigeuchi, N. Yanagizawa, H. Nitta, and S. Tomura, "Variable coupling coefficient integrated inductor," *IEEE Trans. Ind. Appl.*, vol. 60, no. 1, pp. 773–782, Jan./Feb. 2024.

[15] C. Li, L. Wang, G. Zheng, M. Fu, and H. Wang, "Small-signal modeling and loop analysis of ultrafast series capacitor trans-inductor voltage regulator with constant on-time control," *IEEE Trans. Power Electron.*, vol. 40, no. 2, pp. 3262–3274, Feb. 2025.